

METHODS AND RESOURCES

Sensory Processing

Unified measures quantifying intensity and similarity of pain and somatosensory percepts

✉ Eric J. Earley,^{1,2,3} ✉ Malin Ramne,³ and ✉ Johan Wessberg⁴

¹Department of Orthopedics, University of Colorado Anschutz Medical Campus, Aurora, Colorado, United States; ²Bone-Anchored Limb Research Group, University of Colorado Anschutz Medical Campus, Aurora, Colorado, United States;

³Department of Electrical Engineering, Chalmers University of Technology, Gothenburg, Sweden; and ⁴Department of Physiology, Institute of Neuroscience and Physiology, Sahlgrenska Academy, University of Gothenburg, Gothenburg, Sweden

Abstract

Across somatosensory and pain literature, there exist several methods of characterizing the location and extent of perceived sensations, and quantifying how these sensory maps may differ. However, these measures of somatosensory intensity and similarity can give non-unique results, creating challenges in literature review and meta-analysis across different methods. In this paper, we propose novel and unifying measures to quantify the similarity and intensity of pain maps and somatosensory percepts. These measures are generalizable and can be applied to any application of somatosensory maps and are usable with both discretized and free-hand drawings in both two-dimensional and three-dimensional representations. Somatosensory percept intensity (SPI) is inspired by Piper's law, which describes the phenomenon of incomplete spatial summation wherein changes in pain area do not yield linearly proportional changes in perceived intensity. Somatosensory percept deviation (SPD) is derived from optimal transport theory, which quantifies differences between two probability distributions or somatosensory maps. Mathematical derivations for both measures are provided. The utility of these measures is demonstrated using data from two studies, one characterizing elicited somatosensory percepts, and one investigating neuropathic pain drawings. The proposed measures strongly agree with the validation studies, illustrating their potential as agnostic measures for characterizing somatosensory percepts in studies and meta-analyses. Ultimately, our work yields powerful unified measures for use in the fields of perception and pain and may aid in improved pain characterization within healthcare, granting a better understanding of the needs and progression of patients experiencing pain.

NEW & NOTEWORTHY We propose novel and unifying measures to quantify the similarity and intensity of pain maps and somatosensory percepts. These measures are generalizable and applicable to any application of somatosensory maps, resulting in improved pain characterization within healthcare and better understanding of the needs and progression of patients experiencing pain.

pain intensity; pain map; pain measure; percept; somatosensory

INTRODUCTION

The mapping of localized sensations felt on the body is of significant interest in both clinical and scientific circles. Pain maps are commonplace in clinical evaluation and treatment of chronic pain, such as fibromyalgia, spinal cord injury, and low back pain (1–6). In neuroscience research, advancements in peripheral nerve stimulation have led to many studies characterizing sensations elicited from such stimulation

(7–11). In both cases, these somatosensory maps can localize nociceptive or non-nociceptive sensations via “free-hand” drawings or by indicating distinct regions on the body, which may be further discretized into subregions or uniform grids (Fig. 1). The variety of maps results in a corresponding variety of methods to quantify “similarity;” regions or grids may be compared using the number of stable sites (9), whereas similarity between free-hand drawings may use image processing algorithms (12, 13) or the Jaccard similarity



Correspondence: E. J. Earley (eric.earley@cuanschutz.edu).

Submitted 22 January 2025 / Revised 2 March 2025 / Accepted 11 June 2025



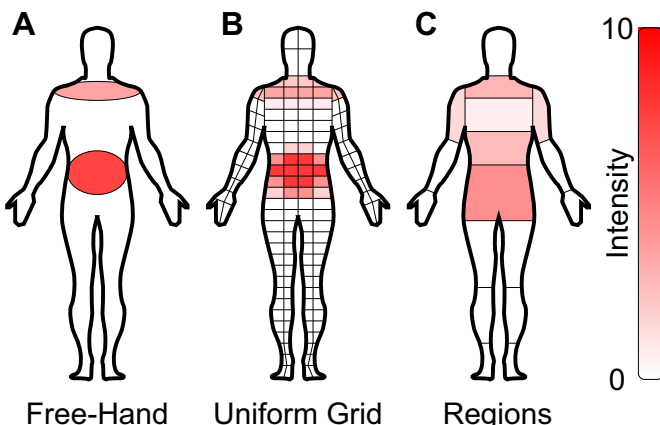


Figure 1. Pain maps and somatotopic maps can take on many forms, which can make cross-study comparisons challenging. Using a hypothetical instance of an individual indicating shoulder and back pain, we illustrate the differences between somatotopic maps recorded as free-hand drawings (*A*), a uniform grid (*B*), and body regions (*C*). In all instances, the sensible area is considered to be the extent of the body map, whereas the perceptive field is considered to be all areas where sensation is currently felt, with a corresponding intensity provided for each element of the perceptive field. The goal of the proposed measures is to describe differences between two perceptive fields in such a way as to consider both intensity and location, and such that results can be compared irrespective of recording method.

coefficient (5, 14–16). This variety can make comparison between studies difficult, even those that evaluate the same sensations.

The intensity of pain or sensations also features a wide variety of quantitative metrics. For pain, especially, these metrics tend to be acquired via questionnaire, typically using quantitative rating scales such as the numeric rating scale (NRS), visual analog scale (VAS), and Likert scale (17, 18). However, these measures alone are unable to decouple between the spread and the intensity of somatosensory percepts or quantify the change of pain intensity in different regions of the affected area in the context of pain. Hence, a measure for precisely quantifying the intensity of sensations could be helpful for tracking progress and outcomes of pain interventions, as patients often struggle to articulate the nuances of their pain experience (19). Having a quantifiable measure of pain intensity beyond the NRS, VAS, and Likert scales may allow for clearer communication between patients and healthcare providers, leading to better-informed decisions and care. Measures of pain intensity and spatial spread can also generate quantifiable feedback on the outcome of treatment decisions and can help optimize treatment plans and reduce unnecessary procedures or medications, potentially saving costs associated with pain management while improving outcomes for patients.

Another limitation of existing measures of similarity and intensity is that their behavior can be inconsistent in certain conditions. For example, measuring the similarity as the number of stable sites (9) will calculate less similarity if two percept fields are farther apart, but only if there is at least some overlap. If the fields share no common areas within the somatosensory map, then fields located close to each other will yield the same outcome as fields that are farther away. This inconsistency can, in some applications, complicate the

interpretation of analyses made using these measures; thus, there is a need for a new set of measures with consistent behavior across conditions.

In this manuscript, we propose novel and unifying measures to quantify intensity and similarity of somatosensory percepts, termed somatosensory percept intensity (SPI) and somatosensory percept deviation (SPD), respectively. These measures are generalizable and can be applied to any application of somatosensory maps and are usable with both discretized and free-hand drawings in both two-dimensional (2-D) and three-dimensional (3-D) representations. We demonstrate the utility of these measures using data from two separate studies investigating somatosensation and pain using different methods.

MATERIALS AND METHODS

The methods described herein originally arose during the course of research characterizing somatosensory percepts elicited from direct nerve stimulation in persons with upper limb amputation who had been fitted with a neuromusculoskeletal prosthesis (20–22). The process of capturing qualitative descriptions of sensations, as well as understanding their spatial and temporal dynamics, involved frequent and direct involvement with participants, whose input has subsequently guided the somatosensory map framework and measures of intensity and similarity in the following sections.

Assumptions about Somatosensory Maps

Percept field.

We define a percept field as an indication of the regions of the body on which a sensation is felt. Such a percept field is intrinsically bound to what we term the sensible area—the areas of the body capable of sensation in even the slightest degree, or the corresponding phantom representation of a missing portion of the body.

For the calculation of SPI and SPD, we make the following assumptions about percept fields:

- 1) The size of a percept field is greater than zero (e.g., a positive value) in all dimensions of interest.
- 2) The distance between any portion of any two percept fields can be measured or estimated in absolute (positive) units of length.
 - a) For predefined grids and regions, distance (e.g., Euclidean norm) will typically be measured between region centroids or anchor points.
 - b) For free-hand drawn boundaries, the distance between any two points between fields should be measurable.
- 3) The percept field has a discrete and closed boundary, which may be defined by a combination of free-hand drawn boundaries, predefined grids and regions, and the limits of the corporeal body and phantom representation.
- 4) Any perceived sensation is an instantaneous capture of the percept intensity within the percept field and does not account for temporal properties such as transient changes in location or sensation area.

By virtue of *assumptions 1* and *2*, percept fields exist within a space where measurements can be described in terms of units of length, including meters, pixels, or percentage body

height. *Assumption 3* not only bounds percept fields to the sensible area but also prohibits “feathered” borders as are collected via some questionnaires (23); a method to incorporate this “feathered” edge into the SPD measure is described in the APPENDIX. *Assumption 4* limits sensation maps to instantaneous sensations, which allows the quantification of the acute variability and similarity of sensations.

Percept intensity.

We define the percept intensity as the magnitude of a perceived sensation. Such intensity is intrinsically bound to the percept field—all elements of the percept field must be accompanied by a percept intensity.

For the calculation of SPI, we make the following assumptions about percept intensity:

- 5) The percept intensity is greater than or equal to zero for all intensities.
- 6) The working range of percept intensity is finite.
- 7) The numerical measure of percept intensity is transitive across its working range, larger values definitively represent higher percept intensities than smaller values.

Assumptions 5 and *6* ensure that percept intensity can be properly quantified and, along with *7*, ensure the monotonicity of the SPI in relation to the percept intensities of the included percept fields. *Assumption 7*, importantly, does not enforce a particular scaling, such as a linear relationship.

Desired Behavior of Similarity and Intensity Measures

Below, we list the desirable behavior of SPI:

- 1) Minimum intensity is achieved if there is no perceivable sensation within the region of interest (RoI).
- 2) Maximum intensity is achieved if maximum sensation is perceived throughout the entire RoI.
- 3) A larger change in percept intensity yields a larger change in SPI when percept field area is constant.
- 4) A larger change in percept field area yields a larger change in SPI when percept intensity is constant.

Behaviors 1 and *2* define the minimum and maximum limits of percept intensity, whereas *behaviors 3* and *4* align the directionality and ensure monotonicity of the intensity measure.

Here, we list the desirable behavior of a measure of SPD:

- 5) Maximum similarity is achieved if two somatosensory maps are identical.
- 6) A larger change in percept field area yields a larger reduction in similarity.
- 7) A larger change in percept field position yields a larger reduction in similarity.

Behavior 5 defines the concept of similarity as the degree of agreement between two maps, whereas *behaviors 6* and *7* align the directionality and ensure monotonicity of the similarity measure.

Derivation of Measures

Percept map.

Let $\mathbf{M} \in \mathbb{R}^N$ represent a percept map existing within an N -dimensional somatosensory map (e.g., a 2-D drawing or a 3-D body model). \mathbf{M} can represent a collection of discrete

points (as might be obtained from a somatotopic map divided into regions) or a continuous closed contour (as might be obtained from a free-hand drawn percept field). However, the method used to calculate SPD (defined in the next section) is not analytically tractable in most cases (though a generalization of this approach for continuous regions is described in the APPENDIX), thus continuous closed contours should be discretized into a finite number of elements so that the metric can be calculated via numerical optimization. We therefore let \mathbf{M} comprise a total of n individual regions $M(i)$, each encompassing an N -dimensional area $A(i)$ and with a location described by a single coordinate $\mathbf{x}_i \in \mathbb{R}^N$.

Percept field.

Let $\mathbf{P} \in \mathbf{M}$ represents a measured percept field describing a somatosensory or pain experience. Each region of percept field $P(i)$ is defined as the instantaneous sensation intensity for which $0 \leq P(i) \leq P_{\max}(i)$, where $P_{\max}(i)$ is the maximum intensity that can be felt in that region; for regions outside of the somatotopic map or regions that are completely desensitized, $P_{\max}(i) = 0$, otherwise $P_{\max}(i)$ will depend on the limits of the intensity scale used (e.g., 10 on a 10-point NRS) and the level of desensitization in the region.

Somatosensory percept intensity.

SPI encompasses the total “amount” of sensation perceived by a person. It can be thought of as a weighted sum of the quantified sensation intensities (e.g., as captured by an NRS) and the areas that each sensation is felt across (Fig. 2A). The calculation of SPI is inspired by Piper’s law, which describes spatial and temporal summation of luminance thresholds in peripheral vision (24, 25). The same patterns of spatial and temporal summation have also been noted in pain evoked by mechanical pressure (26). One phenomenon that arises from this prior research is the notion of incomplete summation, where changes in stimulus area do not result in a linearly proportional change in perceived intensity, which has been observed in vision (27–29). It is possible that the same phenomenon occurs in somatosensory stimuli, though to our knowledge, no study has yet investigated this.

We calculate SPI as:

$$SPI = \sum_i^n P(i) \cdot \left(\frac{A(i)}{\hat{A}} \right)^k \cdot \hat{A} \quad (1)$$

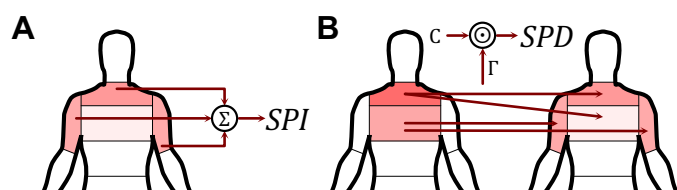


Figure 2. Intensity and similarity measures presented here can be calculated from somatotopic and pain maps. **A:** somatosensory percept intensity (SPI) is a weighted sum of the intensity of a sensation in a region and the size of that region. **B:** somatosensory percept deviation (SPD) is the element-wise product (\odot) of the transportation plan Γ (describing the percept intensity changes from one percept field to another) and the transportation cost \mathbf{C} .

where \hat{A} is the unit area. Recall that $P(i)$ and $A(i)$ are the instantaneous sensation intensity and area of the i^{th} region of the percept map \mathbf{M} . We include a summation coefficient k in *Eq. 1* to account for the possibility of incomplete summation. The summation coefficient can range from 0 to 1, asserting different assumptions upon the system or simplifying calculations. A summation coefficient of 0, for example, may be used if all regions are of equal size (or otherwise carry equal weight) to effectively remove $A(i)$ from the equation, whereas a summation coefficient of 1 assumes complete spatial summation. As summation coefficients may vary widely between applications, we recommend the default value of $k = 0.5$ commonly cited in literature (24, 25) unless prior research suggests the use of a different coefficient.

The units of SPI are the product of the units of the sensation intensity and the area. These units allow for intuitive interpretation of the outcome within the context of its measurement; however, it can make comparison difficult between studies using different measures of intensity. In such instances where comparison is desired, the normalized SPI (nSPI) can be calculated as:

$$nSPI = \sum_i^n \frac{P(i)}{P_{\max}(i)} \cdot \left(\frac{A(i)}{\hat{A}} \right)^k \cdot \hat{A} \quad (2)$$

Defining SPI and nSPI in this way ensures that total experienced sensation scales according to both instantaneous sensation intensity and percept field area. nSPI also ensures parity between studies using different scales and allows for the use of biological markers as a quantitative measure of intensity (e.g., afferent nerve or cortical activity magnitudes).

Somatosensory percept deviation.

Given two somatosensory maps (e.g., two pain maps recorded at different times), SPD quantifies the degree of difference between the maps. The amount of deviation between the two maps is, by definition, inversely related to the similarity of the maps (*Fig. 2B*). To ensure compliance with the aforementioned assumptions and behaviors, SPD is based on optimal transport theory (OTT), which strives to quantify “distance” between two probability distributions. In this case, we define the “probability distribution” as the indicated percept field, and thus OTT quantifies the “distance” between two percept fields. Specifically, SPD uses the Wasserstein metric to quantify the dissimilarity between two percept fields (30, 31); this metric has seen similar use to explain dissimilarity between stochastic neural representations (32) and to classify prosthetic limb movements by comparing high-density EMG images to determine EMG maps with the greatest degree of similarity (33).

For SPD, the objective of OTT is to minimize the “cost” of transforming one percept field \mathbf{P}_1 into another \mathbf{P}_2 . The transportation cost \mathbf{C} is typically simply the Euclidean distance between regions i and j :

$$C(i,j) = \|\mathbf{x}_j - \mathbf{x}_i\|_2 \quad (3)$$

This Euclidean distance can be defined in any units of length (e.g., millimeters or pixels), however to facilitate the greatest degree of comparison between applications, we recommend normalizing the distance by using the 50th-percentile dimensions of the ROI, defined in anthropometric tables

(34, 35), as a normalizing factor by which to divide the measured lengths of the somatotopic map.

The process of transforming \mathbf{P}_1 into \mathbf{P}_2 , each comprising n regions, can be defined as the transportation plan Γ , which takes the form of an $n \times n$ matrix where each element $\Gamma(i,j)$ describes the quantity transferred from \mathbf{x}_i to \mathbf{x}_j . For Γ to be valid for OTT, it must satisfy the following constraints:

$$\sum_j^n \Gamma(i,j) = \frac{P_1(i) \cdot A(i)^k}{SPI_1} \quad \forall i \in [1, \dots, n] \quad (4)$$

$$\sum_i^n \Gamma(i,j) = \frac{P_2(j) \cdot A(j)^k}{SPI_2} \quad \forall j \in [1, \dots, n] \quad (5)$$

The normalizations by SPI_1 and SPI_2 ensure that the total transported quantity is equivalent. This normalization can also be achieved by defining the normalized percept field as:

$$\mathbf{Q} = \frac{\mathbf{P} \odot \mathbf{A}^k}{SPI} \quad (6)$$

where \odot denotes the element-wise product. Applying *Eq. 6* to *Eqs. 4* and *5* yields the following constraint equations:

$$\sum_j^n \Gamma(i,j) = Q_1(i) \quad \forall i \in [1, \dots, n] \quad (7)$$

$$\sum_i^n \Gamma(i,j) = Q_2(j) \quad \forall j \in [1, \dots, n] \quad (8)$$

These constraints ensure that the total quantity transported out of $Q_1(i)$ is equal to the quantity contained within $Q_1(i)$, and that the total quantity transported into $Q_2(j)$ is equal to the quantity contained within $Q_2(j)$.

The final constraint pertains to the transportation plan Γ , which cannot include negative values:

$$\Gamma(i,j) \geq 0 \quad \forall (i,j) \in [1, \dots, n] \quad (9)$$

The total cost of executing transportation plan Γ can be calculated via element-wise product with the transportation cost \mathbf{C} . Formatting this as an optimization problem thus takes the form:

$$\underset{\Gamma}{\text{minimize}} \quad \Gamma \odot \mathbf{C} = \sum_i^n \sum_j^n \Gamma(i,j) \cdot C(i,j) \quad (10)$$

$$\text{subject to} \quad \Gamma \cdot \mathbf{J}_{n,1} = \mathbf{Q}_1, \quad \Gamma^\top \cdot \mathbf{J}_{n,1} = \mathbf{Q}_2, \quad \Gamma \geq 0 \quad (11)$$

where $\mathbf{J}_{n,1}$ is an $n \times 1$ matrix of ones.

The estimated optimal transportation plan $\hat{\Gamma}^*$ is then used to calculate SPD:

$$SPD = \hat{\Gamma}^* \odot \mathbf{C} = \sum_i^n \sum_j^n \hat{\Gamma}^*(i,j) \cdot C(i,j) \quad (12)$$

A smaller SPD outcome is associated with a greater degree of similarity between the somatotopic maps for percept fields \mathbf{P}_1 and \mathbf{P}_2 .

The term “deviation” is also appropriate in this context, as the unit of an SPD measure is the same as the units of the transportation cost \mathbf{C} . Furthermore, it can be shown that SPD of a purely translational difference between \mathbf{P}_1 and \mathbf{P}_2 is simply the magnitude of the translation.

Although it was not listed as a required behavior for similarity measures, one desirable property of SPD is its symmetry ($SPD(\mathbf{P}_1 \rightarrow \mathbf{P}_2) = SPD(\mathbf{P}_2 \rightarrow \mathbf{P}_1)$).

Validation of Measures

To demonstrate the use of SPD as a similarity measure, we applied SPD to somatosensory data from two different studies. These studies were selected to represent a variety of somatosensory map styles, bodily RoIs, subject populations, and research purposes. For each study, SPD is used to quantify similarity between somatosensory percepts and subsequently compare this result to those reported in the original study. The expectation is not that outcomes are identical; rather, SPD is expected to generally align with the original outcomes while simultaneously providing novel insights to support hypotheses that the original methods may not have been able to elucidate.

SPI and SPD were calculated using custom MATLAB scripts. Constrained nonlinear function optimization (used for *Eqs. 10* and *11*) was conducted using the *fmincon* function included in MATLAB's *Optimization Toolbox* (36). Researchers using Python may consider the *wasserstein_distance_nd* function included in the *scipy* library (37), and those using R may consider the *Wasserstein* function included in the *transport* package (38); regardless of the program used, researchers need only define the transportation cost \mathbf{C} to implement this method.

Use of stimulation waveform shapes to elicit different somatosensory percepts.

In this study by Collu et al. (11), transcutaneous electrical nerve stimulation (TENS) of the median nerve elicited sensations on the palms of the hands of 11 able-bodied individuals. The shapes of the stimulation waveforms were changed between various current profiles, and the location of the elicited sensation was recorded using a custom graphical interface. This interface allowed participants to encircle the area on the palm where a sensation was felt, after which the application would fit a bivariate normal distribution (appearing as an ellipse) to the indicated points. Participants were also asked to describe the quality, intensity, diffuseness, depth, dynamics, and naturalness of the elicited sensation. Although intensity was not evaluated in the study, the change in perceptive field area was investigated, showing that perceptive fields elicited by nonrectangular waveforms generally grew in area compared with rectangular waveforms, though these differences were not statistically significant.

SPD was used to quantify the differences in sensation intensity and percept fields between the five stimulation

waveform shapes included in the study. This analysis included the intensity $P(i)$ omitted from the original study, which was measured using a VAS. Statistical comparisons were made using Wilcoxon's signed rank test. The original study was approved by the Swedish regional ethical committee in Gothenburg (Dnr: 2019-05,446) and the research was performed in accordance with the relevant guidelines and regulations in compliance with the Declaration of Helsinki.

Reliability of pain drawings of spinal cord injury neuropathic pain.

In this study by Rosner et al. (6), 20 individuals with spinal cord injury (SCI) indicated areas in which they felt neuropathic pain by drawing on a ventral/dorsal body chart printed on a sheet of paper. These drawings were then digitally scanned, and the shaded regions indicating pain were overlaid atop a standardized dermatome grid (2). Average pain intensity during the last week was measured using an NRS (0–10). This process was then repeated approximately 2 wk later, and the two pain maps were compared using inter-class correlation coefficients, showing good agreement for both pain extent and intensity between measurements.

The test-retest reliability was reanalyzed using SPD to investigate the degree of agreement for measures unifying both pain extent and pain intensity. No difference in outcome was expected, as test-retest reliability of pain extent and pain intensity was excellent in the original study, with very low bias. Instead, the importance of validation using this study was to demonstrate the reliability of the numerical optimization methods used for *Eqs. 10* and *11*. The original study was approved by the local ethics board, "Kantonale Ethikkommission Zürich" (reference number: EK-04/2006).

RESULTS

Comparison with Existing Methods

For somatosensory intensity, we compared SPI to existing quantitative rating scales commonly used for assessing pain intensity (such as VAS, NRS, and Likert scales) (Table 1). Both methods will fulfill behaviors 1 and 3, but the quantitative rating scales do not fulfill behaviors 2 and 4. The quantitative rating scales are independent of the location and size of the percept field, thus maximum intensity can be achieved regardless of the size of the percept field. Furthermore, while it is likely that respondents may indicate a higher percept intensity using a quantitative rating scale when the percept field is larger, this would likely be more closely related to ambiguous or imprecise instructions given to the respondent

Table 1. Somatosensory percept intensity compared with existing methods

Behavior	Quantitative Rating Scale	Somatosensory Percept Intensity (SPI)
1) Minimum intensity is achieved if there is no perceivable sensation within the region of interest (RoI)	✓	✓
2) Maximum intensity is achieved if maximum sensation is perceived throughout the entire RoI	✗	✓
3) A larger change in percept intensity yields a larger change in overall intensity when percept field area is constant	✓	✓
4) A larger change in percept field area yields a larger change in overall intensity when percept intensity is constant	✗	✓

Table 2. Somatosensory percept deviation compared with existing methods

Behavior	Change in Area	Overlapping Area/Stable Sites	Structural Similarity Index	Jaccard Similarity Coefficient	Somatosensory Percept Deviation (SPD)
5) Maximum similarity is achieved if two somatosensory maps are identical	✓	✓	✓	✓	✓
6) A larger change in percept field area yields a larger reduction in similarity	✓	?	✓	✓	✓
7) A larger change in percept field position yields a larger reduction in similarity	X	?	?	?	✓

when reporting their perceived sensation, rather than a feature of the scale itself as a reporting method. Only the SPI is guaranteed to fulfill all four behaviors.

We then examined how well the desired behaviors (see *Desired Behavior of Similarity and Intensity Measures*) are fulfilled by existing measures of similarity (change in area, overlapping area/stable sites, structural similarity index, and Jaccard similarity coefficient) and by our novel proposed measure, SPD. For somatosensory map location and area (**Table 2**), *behavior 5* is fulfilled by all five methods, but *behavior 6* is not guaranteed when measuring the overlapping area or number of stable sites, as a larger percept field which completely overlaps a smaller field will have the same overlapping area regardless of the size difference. *Behavior 7* can never be captured when only measuring the change in percept area and is not guaranteed when measuring overlapping area, structural similarity index, or Jaccard similarity coefficient (specifically, when both sensory maps do not overlap). Only the SPD is guaranteed to fulfill all three behaviors.

SPI and SPD Validation

Stimulation waveform shapes.

Figure 3 shows the SPI for sensations elicited by single pulses or trains of pulses of different neurostimulation waveform shapes computed using data originally reported on in a study by Collu et al. (11) involving TENS of the median nerve. As expected, SPI is generally higher for stimulation pulse trains than for single pulses due to the larger areas of the elicited percepts. Percept intensities tended to be lowest for rectangular waveforms (which deliver the lowest current while maintaining the same overall charge injection) and highest for triangular waveforms (which deliver the highest current for a given charge delivery). Although percept

intensity was not investigated in the original study, these trends align with the lower rheobasic currents identified for nonrectangular waveforms and the higher sensitivity to pulse current compared with pulse duration (22); however, no significant differences in percept intensities were found between waveform shapes for either single pulses ($P \geq 0.0537$) or for pulse trains ($P \geq 0.0537$) of suprathreshold stimuli.

Figure 4 shows the SPD between somatosensory maps elicited by different neurostimulation waveform shapes. Somatosensory maps (*inset*), which were more dissimilar resulted in a higher percept deviation. For single pulses (lilac), percept deviations between triangular and linear increasing waveforms were smaller than deviations between rectangular and triangular waveforms ($P = 0.032$), and deviations between sinusoidal and triangular waveforms ($P = 0.042$). For pulse trains (green), percept deviations between triangular and linear waveforms were significantly smaller than deviations between rectangular and triangular waveforms ($P \leq 0.042$). These results support the hypothesis that waveforms with equivalent delivered charge and peak current (triangular and linear) are more similar than waveforms with equivalent delivered charge but lower peak currents (rectangular and sinusoidal). However, most other comparisons were not significantly different.

Neuropathic pain drawings.

Figure 5 shows the outcomes of the proposed metrics (SPI and SPD) compared with the outcomes reported in the original study (neuropathic pain extent and intensity) (6). The scatter plots (three left plots) show the mean neuropathic pain extent (e.g., the percentage of the body on which pain was indicated), mean neuropathic intensity (NRS scale 0–10), and SPI, and their relations to SPD. Across all three

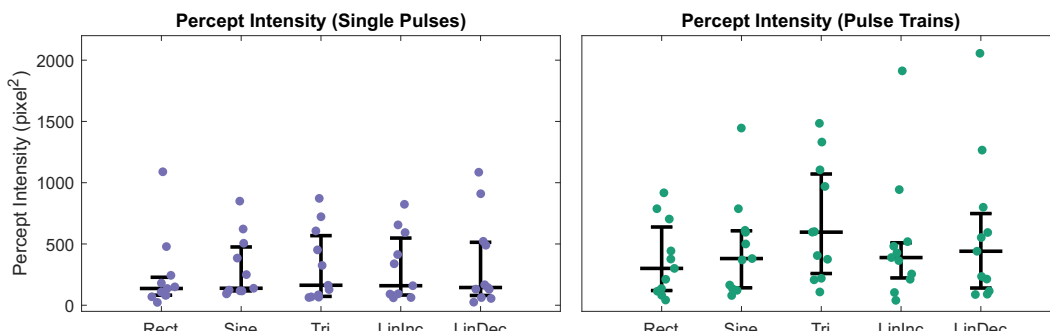


Figure 3. Percept intensities for sensations elicited by different neurostimulation waveform shapes ($n = 11$), delivered as either single pulses (lilac) or as trains of pulses (green). Whiskers depict medians and quartiles.

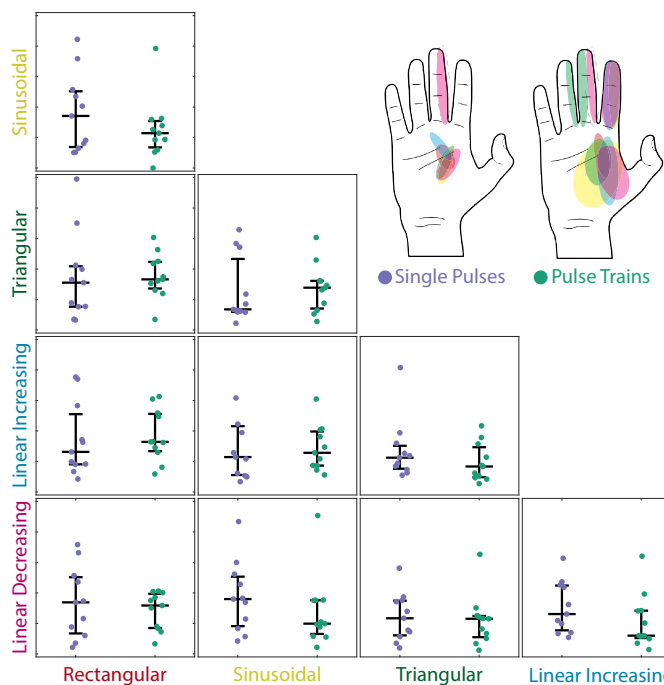


Figure 4. Percept deviation between somatosensory maps elicited by different neurostimulation waveform shapes (inset, top-right), delivered as either single pulses (lilac) or as trains of pulses (green). Percept deviations range from 0 to 250 pixel-units in the plots shown ($n = 11$). Whiskers depict medians and quartiles.

metrics, there appears to be no clear trend, suggesting independence of the SPD from pain extent and pain intensity separately, and from SPI (which, in essence, is jointly influenced by pain extent and intensity). However, it should be noted that, unlike in the original study, all SPD values were greater than zero (because SPD measures the magnitude of difference between pain maps, not the increase or decrease in SPI).

The right plot shows the intraclass correlation coefficients (ICCs) for neuropathic pain extent and intensity (which are reported in the original study) and for SPD,

evaluated for pain assessed at two different points in time. All three metrics showcase a strong degree of ICC, indicating strong agreement between test and retest outcomes. Furthermore, ICCs for SPD were generally calculated as between the values obtained for pain extent and pain intensity, and SPD demonstrated slightly less variability between participants than pain intensity. That said, it is worth noting that both of these observations are largely dependent on the summation coefficient k . Nonetheless, we found that the proposed measures agree strongly with the findings of the original study.

DISCUSSION

Here, we propose a set of unifying measures that aim to quantify the similarity and intensity of somatosensory percepts. Our intent was to develop measures that are generalizable to the methods which are used to capture these somatosensory maps, be they discretized or continuous in nature (Fig. 1). After defining the design criteria and deriving SPD and SPI, we validate the measures by reanalyzing data from two studies using two different methods of somatosensory mapping.

In the first study, percept fields were drawn to indicate the perceived sensations elicited from TENS of the median nerve in 11 subjects. The original study only compared perceptive field area between stimulation conditions, but by analyzing the same data using SPD, we were able to quantify not only the differences in percept field area but also location. The importance of this distinction can be seen when comparing the results of the original study to the results presented here. Percept intensities were, as expected, higher for stimulation pulse trains than for single pulses (Fig. 3); however, the deviation between percept fields was smaller for pulse trains. This suggests that the percept fields for single pulses were less stable between stimulation conditions, which may be due to percept field saturation for pulse trains.

In the second study, locations of neuropathic pain were recorded from 20 individuals twice, and the percept fields

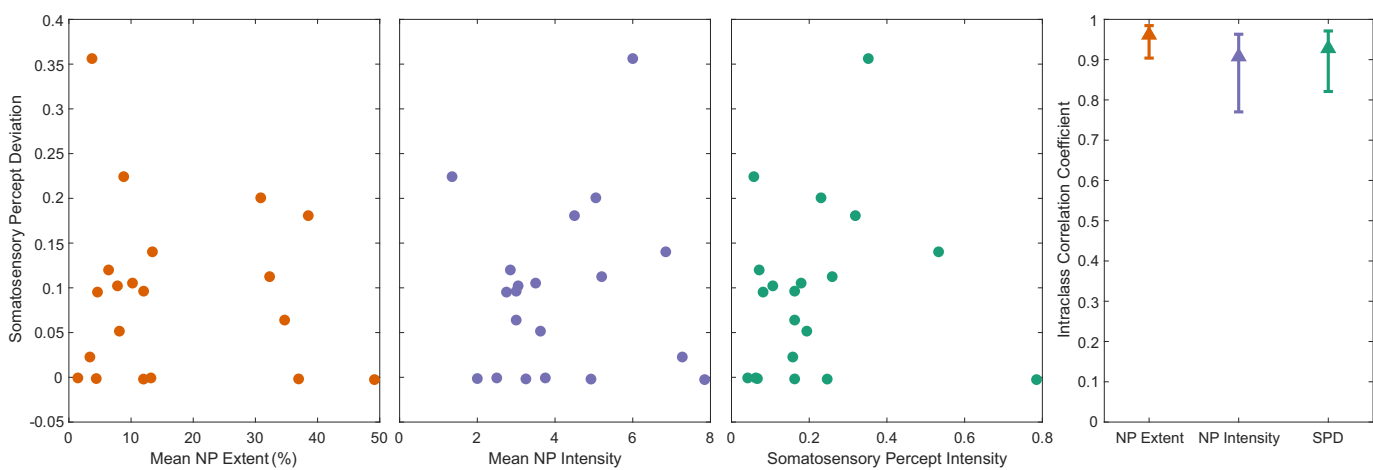


Figure 5. Scatter plots ($n = 20$) illustrate the general independence of the neuropathic pain (NP) extent and intensity, and the SPI, from the SPD (left plots). The intraclass correlation coefficient (right plot) also showed no major differences between the metrics of NP extent, NP intensity, and SPD. Whiskers depict medians and quartiles.

were segmented into regions using a dermatome grid. The size of the percept field was quantified as the extent of the marked areas, as a percentage of the total area, and intensity was measured with a Likert scale. Measuring repeatability of neuropathic pain using SPD yielded a similar intraclass correlation coefficient to using the original measures, overall demonstrating agreement with the original study.

In studies, pain is often reduced to one or a handful of numbers as the proxy for the intensity and unpleasantness of certain aspects of the pain. In reality, pain is a complex and highly subjective experience, encompassing myriad sensation qualities. Furthermore, pain resulting from an injury or lesion can spread to secondary locations through processes of peripheral and central sensation (39). The quality and intensity of such “referred” pain can differ significantly from the local pain at the location of the injury, and importantly, the underlying mechanism of the referred pain can be separate from the cause of local pain (40). Different pain interventions target different mechanisms, and thus, referred and local pain may be differentially affected (39). Evaluating pain as a single point on an NRS may not capture changes in pain intensity at different sites, and thus may not accurately reflect the change in sensation. Incorporating this type of measure in future pain studies could provide insight into the differential mechanisms of different pain sensations and treatments.

As illustrated in Fig. 1, SPI and SPD can be used irrespective of the somatosensory map that is used for measurement. In addition to the versatility that this provides for longitudinal clinical or scientific monitoring, a map-agnostic somatosensory measure facilitates broader meta-analyses across studies, which use different somatosensory maps and percept intensity scales, though these comparisons should not be considered perfect. First, differences in somatosensory maps will result in differences in resolution, which in turn will cause differences in SPI and SPD due solely to the distribution of regions. Second, users of different somatosensory maps may define their percepts differently depending on how they view the maps or the interface on which they are provided; for example, respondents may be tempted to only indicate one percept region if the subdivisions are very large, even if they truly feel a percept at the intersection between two regions. Alternatively, because of the number of regions in a grid map, respondents may not (or may not be able to) indicate different percept intensities for each region separately. Changes in behavior due to the somatosensory map are a topic of future investigation, but nonetheless may be an acceptable compromise for the ability to synthesize results across multiple studies.

Another application of this measure could be in the realm of sensory phenotyping of pain, in which researchers and clinicians try to match sensory symptoms to pain mechanisms to better predict treatment responses of individual patients (41, 42). These sensory symptoms include, among other things, the intensity of different sensation qualities and how the intensity varies over time. SPD could add more nuance and information to this type of measure by also

incorporating how the spatial spread of pain varies, and thus might allow for more accurate predictions of pain mechanism and treatment outcome.

In summary, we demonstrate that outcomes calculated using SPI and SPD are in agreement with the measures used in these different studies and can even provide new insights not available through other measures (as was the case with the neurostimulation study). Furthermore, SPI and SPD exhibit all of the desired behaviors listed in Tables 1 and 2. Thus, we believe SPI and SPD to be useful measures for studies involving the quantification of somatosensory percepts and how they may differ between conditions, providing unifying metrics comprising somatosensory percept intensity and deviation.

Limitations

SPD has a computational complexity of up to $O(n^3 \log n)$ (43), which can be prohibitively costly for somatosensory maps with many regions. The use of techniques such as entropic regularization has been proven to lower the computational complexity to nearly $O(n)$ (44). Furthermore, the scope of the optimization can be reduced by removing regions P not contained in either \mathbf{P}_1 or \mathbf{P}_2 .

The use of numerical rating scales or other subjective quantitative scales of pain has well-known limitations, particularly when it comes to reliability of responses and accuracy of pain memory (45, 46). Furthermore, the potential nonlinearity of such psychometric scales creates challenges when comparing sensations measured across time, at different bodily locations, and between individuals. Despite these limitations, these pain assessment tools are prevalent throughout numerous pain pathologies and are frequently standard of care within medicine (47). Our unified pain measures were developed assuming these standardized clinical practices, despite the aforementioned limitations, however, the derivation of SPI and SPD is intentionally nonprescriptive so that other future measures and instruments could be used instead.

We note that SPI and SPD do not require a particular scaling of the tool used to collect the data on which the measures are computed, only that it is transitive across its working range. This means that the measures can be computed on data collected on ordinal, interval, and ratio scales. Furthermore, we leave open the possibility of incorporating more sophisticated psychophysical models into the calculation of SPI in cases where more is known about the sensory modality. For example, if sufficient experimentation has been conducted to estimate the proportionality and exponential constants α and β , Stevens' power law (48) can be incorporated into the calculation of nSPI as follows:

$$nSPI = \sum_i^n \alpha \left(\frac{P(i)}{P_{\max}(i)} \right)^\beta \cdot \left(\frac{A(i)}{\hat{A}} \right)^k \cdot \hat{A} \quad (12)$$

However, as these constants may be dependent upon numerous other factors (49), this level of complexity should be reserved for well-studied and understood applications. We furthermore note that, due to the inherently judgmental nature of subjective magnitude estimation, comparisons of SPI and SPD between different sensory modalities (e.g., phantom limb pain and back pain) should be pursued with caution and considered exploratory.

There is great interest in identifying objective measurements of pain. In research, neurologically derived signals are being used to decode somatosensory intensity, for example, resulting from tactile stimulus (50). Other techniques proposed in research studies to quantify somatosensory intensity include heart rate variability (51) and fMRI (52). Despite the numerous limitations and lack of validation preventing these approaches from being used in clinical practice, these types of objective measures could be used for the purposes of calculating SPI and SPD. Furthermore, these techniques may not be as suitable for clinical practice owing to the requirement of additional, and sometimes expensive, sensors.

Conclusions

In this study, we introduce two new measures, somatosensory percept intensity (SPI) and somatosensory percept deviation (SPD), to better quantify the intensity and similarity of somatosensory percepts. These measures overcome several limitations of existing methods and can be applied to both pain and somatosensory maps. SPI and SPD fulfill all desired behaviors for similarity and intensity metrics and offer a unified approach to evaluating somatosensory percepts, which can improve the characterization of nociceptive and non-nociceptive sensory experiences and clinical outcomes, ultimately serving as the basis to create powerful new tools for researchers and clinicians alike.

APPENDIX

Generalized Definition of Measures

Let $M \in \mathbb{R}^N$ represent a percept field existing within an N -dimensional somatosensory map. Each region $M(x)$ is defined as the instantaneous sensation intensity $P(x)$ felt at a region with N -dimensional area $A(x)$, for which $0 \leq P(x) \leq P_{\max}(x)$, where: $P_{\max}(x)$ is the maximum intensity that can be felt in that region; for regions outside of the somatotopic map or regions that are completely desensitized, $P_{\max}(x) = 0$, otherwise $P_{\max}(x)$ will depend on the level of desensitization in the region and the limits of the intensity scale used (e.g., 10 on a 10-point NRS).

Somatosensory percept intensity.

We then calculate SPI as:

$$SPI = \int P(x)A(x)^k dx \quad (A1)$$

Defining SPI in this way ensures that total experienced sensation scales according to both instantaneous sensation intensity and percept field area.

Somatosensory percept deviation.

Instead of a transportation plan Γ describing transport from one element to another, Γ is now a transportation field between percept fields \mathbf{P}_1 and \mathbf{P}_2 . Calculating SPD now takes the form of the optimization problem:

$$\underset{\Gamma}{\text{minimize}} \quad \Gamma \odot \mathbf{C} = \sum_i^n \sum_j^n \Gamma(i,j) \cdot C(i,j) \quad (A2)$$

$$\text{subject to } \int_{\mathbf{y}} \Gamma(\mathbf{x}, \mathbf{y}) dx = \int_{\mathbf{x}} Q_1(\mathbf{x}) dx \quad (A3)$$

$$\int_{\mathbf{x}} \Gamma(\mathbf{x}, \mathbf{y}) dx = \int_{\mathbf{y}} Q_2(\mathbf{y}) dy \quad (A4)$$

$$\Gamma \geq 0 \quad (A5)$$

The optimal transport plan can once again be used to calculate SPD:

$$SPD = \hat{\Gamma}^* \odot \mathbf{C} = \iint_{\mathbf{x}, \mathbf{y}} \hat{\Gamma}^* \cdot \mathbf{C} \quad (A6)$$

Extensions

There may be applications where a uniform transportation cost \mathbf{C} is not desired when comparing somatosensory maps. For example, a study investigating selectivity of direct nerve stimulation to elicit tactile sensations may want to consider the mechanoreceptor density of the distal limb. In such a case, the transportation cost can be modified to better account for the variables of interest, for example, by scaling the transportation cost inversely proportional to the two-point discrimination performance.

Sometimes, when defining the perceived locations of perceptions elicited from neurostimulation, the diffuseness of the sensation is also recorded, allowing for the subject to indicate whether the borders of the sensation are well-defined or “feathered.” This diffuseness could interfere with *assumption 3*, which states that percept fields must have a discrete border. However, the diffuseness of a sensation can be accounted for by introducing a diffuseness variable β to the definition of a modified percept field \mathbf{P}' , such that:

$$\mathbf{P}'(i) = P(i) \left(\beta + (1 - \beta) \left(e^{-\frac{1}{2}(\mathbf{x}_i - \boldsymbol{\mu})^\top \Sigma^{-1} (\mathbf{x}_i - \boldsymbol{\mu})} \right) \right) \quad (A7)$$

In other words, the modified sensation intensity is a diffuseness-weighted average between a uniform distribution (i.e., a Dirac measure) and a normalized bivariate Gaussian distribution, scaled by the original sensation intensity $P(i)$. It should be noted that, although $\mathbf{P}' \leq \mathbf{P}$, SPD will remain unchanged due to the normalization in *Eq. 6*.

GLOSSARY

$A(i)$	Area of percept map region $M(i)$
\hat{A}	Unit area
\mathbf{C}	Transportation cost
\mathbf{J}	Matrix of ones
k	Summation coefficient
\mathbf{M}	Percept map
$nSPI$	Normalized somatosensory percept intensity
\mathbf{P}	Percept field
\mathbf{P}'	Percept field of instantaneous sensation intensities within percept map \mathbf{M}
$P_{\max}(i)$	Maximum sensation intensity of percept field region $P(i)$
SPI	Somatosensory percept intensity
SPD	Somatosensory percept deviation
\mathbf{Q}	Normalized percept field

- x_i Coordinate of percept map region $M(i)$
 Γ Transportation plan
 $\hat{\Gamma}^*$ Estimated optimal transportation plan
 \odot Element-wise product

DATA AVAILABILITY

No original data were generated as part of this study. All data used in this study can be requested from the respective corresponding authors (6, 11).

ACKNOWLEDGMENTS

We thank Drs. Jan Rosner and Michèle Hubli for sharing their data on pain drawings for the validation performed in this study (6). We thank Riccardo Collu for his data using stimulation waveform shapes to elicit different somatosensory percepts via TENS (11). We thank Dr. Morten Bak Kristoffersen for his insights in developing the mathematics behind the somatosensory measures. E.J.E. acknowledges Prof. Alex H Williams for his blog post, A Short Introduction to Optimal Transport and Wasserstein Distance (53).

GRANTS

This work was supported by the Promobilia Foundation (Stiftelsen Promobilia), the IngaBritt and Arne Lundbergs Foundation (IngaBritt och Arne Lundbergs Forskningsstiftelse), and the Swedish Research Council (Vetenskapsrådet).

DISCLOSURES

No conflicts of interest, financial or otherwise, are declared by the authors.

AUTHOR CONTRIBUTIONS

E.J.E., M.R., and J.W. conceived and designed research; E.J.E. analyzed data; E.J.E. interpreted results of experiments; E.J.E. prepared figures; E.J.E., drafted manuscript; E.J.E., M.R., J.W. edited and revised manuscript; E.J.E., M.R., J.W. approved final version of manuscript.

REFERENCES

- Ohnmeiss DD. Repeatability of pain drawings in a low back pain population. *Spine (Phila Pa 1976)* 25: 980–988, 2000. doi:[10.1097/00007632-200004150-00014](https://doi.org/10.1097/00007632-200004150-00014).
- Kirshblum SC, Burns SP, Biering-Sorensen F, Donovan W, Graves DE, Jha A, Johansen M, Jones L, Krassioukov A, Mulcahey MJ, Schmidt-Read M, Waring W. International standards for neurological classification of spinal cord injury (Revised 2011). *J Spinal Cord Med* 34: 535–546, 2011. doi:[10.1179/20457721X13207446293695](https://doi.org/10.1179/20457721X13207446293695).
- Brummett CM, Bakshi RR, Goesling J, Leung D, Moser SE, Zollars JW, Williams DA, Clauw DJ, Hassett AL. Preliminary validation of the Michigan Body Map. *Pain* 157: 1205–1212, 2016. doi:[10.1097/j.pain.0000000000000506](https://doi.org/10.1097/j.pain.0000000000000506).
- Barbero M, Fernández-De-Las-Peñas C, Palacios-Ceña M, Cescon C, Falla D. Pain extent is associated with pain intensity but not with widespread pressure or thermal pain sensitivity in women with fibromyalgia syndrome. *Clin Rheumatol* 36: 1427–1432, 2017. doi:[10.1007/s10067-017-3557-1](https://doi.org/10.1007/s10067-017-3557-1).
- Villa MG, Palsson TS, Royo AC, Bjarkam CR, Boudreau SA. Digital pain mapping and tracking in patients with chronic pain: longitudinal study. *J Med Internet Res* 22: e21475, 2020.
- Rosner J, Lütfolf R, Hostettler P, Villiger M, Clijser R, Hohenauer E, Barbero M, Curt A, Hubli M. Assessment of neuropathic pain after spinal cord injury using quantitative pain drawings. *Spinal Cord* 59: 529–537, 2021. doi:[10.1038/s41393-021-00616-6](https://doi.org/10.1038/s41393-021-00616-6).
- Petrini FM, Bumbasirevic M, Valle G, Ilic V, Mijović P, Ćvancara P, Barberi F, Katic N, Bortolotti D, Andreu D, Lechler K, Lesic A, Mazic S, Mijović B, Guiraud D, Stieglitz T, Alexandersson A, Micera S, Raspopovic S. Sensory feedback restoration in leg amputees improves walking speed, metabolic cost and phantom pain. *Nat Med* 25: 1356–1363, 2019. doi:[10.1038/s41591-019-0567-3](https://doi.org/10.1038/s41591-019-0567-3).
- Chandrasekaran S, Nanivadekar AC, McKernan G, Helm ER, Boninger ML, Collinger JL, Gaunt RA, Fisher LE. Sensory restoration by epidural stimulation of the lateral spinal cord in upper-limb amputees. *eLife* 9: e54349, 2020. doi:[10.7554/elife.54349](https://doi.org/10.7554/elife.54349).
- Valle G, Iberite F, Strauss I, D'Anna E, Granata G, Di Iorio R, Stieglitz T, Raspopovic S, Petrini FM, Rossini PM, Micera S. A psychometric platform to collect somatosensory sensations for neuroprosthetic use. *Front Med Technol* 3: 619280, 2021. doi:[10.3389/fmedt.2021.619280](https://doi.org/10.3389/fmedt.2021.619280).
- Aiello G, Valle G, Raspopovic S. Recalibration of neuromodulation parameters in neural implants with adaptive Bayesian optimization. *J Neural Eng* 20: 10.1088/1741-1255/acc975, 2023. doi:[10.1088/1741-2552/acc975](https://doi.org/10.1088/1741-2552/acc975).
- Collu R, Earley EJ, Barbero M, Ortiz-Catalan M. Non-rectangular neurostimulation waveforms elicit varied sensation quality and perceptive fields on the hand. *Sci Rep* 13: 1588, 2023. doi:[10.1038/s41598-023-28594-0](https://doi.org/10.1038/s41598-023-28594-0).
- Wang Z, Bovik AC, Sheikh HR, Simoncelli EP. Image quality assessment: from error visibility to structural similarity. *IEEE Trans Image Process*, 13: 600–612, 2004. doi:[10.1109/tip.2003.819861](https://doi.org/10.1109/tip.2003.819861).
- Osborn LE, Ding K, Hays MA, Bose R, Iskarous MM, Dragomir A, Tayeb Z, Lévy GM, Hunt CL, Cheng G, Armiger RS, Bezerianos A, Fifer MS, Thakor NV. Sensory stimulation enhances phantom limb perception and movement decoding. *J Neural Eng* 17: 056006, 2020. doi:[10.1088/1741-2552/abb861](https://doi.org/10.1088/1741-2552/abb861).
- Jaccard P. Nouvelles Recherches Sur La Distribution Florale. *Bulletin de la Société Vaudoise des Sciences Naturelles* 44: 223–270, 1908. doi:[10.5169/seals-268384](https://doi.org/10.5169/seals-268384).
- Boudreau SA, Kamavuako EN, Rathleff MS. Distribution and symmetrical patellofemoral pain patterns as revealed by high-resolution 3D body mapping: a cross-sectional study. *BMC Musculoskeletal Disorders/BMC Musculoskeletal Disorders* 18: 160, 2017. doi:[10.1186/s12891-017-1521-5](https://doi.org/10.1186/s12891-017-1521-5).
- Leoni D, Falla D, Heitz C, Capra G, Clijser R, Egloff M, Cescon C, Baeyens JP, Barbero M. Test-retest reliability in reporting the pain induced by a pain provocation test: further validation of a novel approach for pain drawing acquisition and analysis. *Pain Pract* 17: 176–184, 2017. doi:[10.1111/papr.12429](https://doi.org/10.1111/papr.12429).
- Jensen MP, Karoly P, Braver S. The measurement of clinical pain intensity: a comparison of six methods. *Pain* 27: 117–126, 1986. doi:[10.1016/0304-3959\(86\)90228-9](https://doi.org/10.1016/0304-3959(86)90228-9).
- Attal N, Bouhassira D, Baron R. Diagnosis and assessment of neuropathic pain through questionnaires. *Lancet Neurol* 17: 456–466, 2018. doi:[10.1016/S1474-4422\(18\)30071-1](https://doi.org/10.1016/S1474-4422(18)30071-1).
- Campbell R, Ju A, King MT, Rutherford C. Perceived benefits and limitations of using patient-reported outcome measures in clinical practice with individual patients: a systematic review of qualitative studies. *Qual Life Res* 31: 1597–1620, 2022. doi:[10.1007/s11136-021-03003-z](https://doi.org/10.1007/s11136-021-03003-z).
- Ortiz-Catalan M, Zbinden J, Millenaar J, D'Accolti D, Controzzi M, Clemente F, Cappello L, Earley EJ, Mastinu E, Kolankowska J, Munoz-Novoa M, Jönsson S, Cipriani C, Sassu P, Brånenmark R. A highly integrated bionic hand with neural control and feedback for use in daily life. *Sci Robot* 8: eadf7360, 2023. doi:[10.1126/scirobotics.adf7360](https://doi.org/10.1126/scirobotics.adf7360).
- Earley EJ, Zbinden J, Munoz-Novoa M, Just F, Vasan C, Holtz AS, Emadeldin M, Kolankowska J, Davidsson B, Thesleff A, Millenaar J, Jönsson S, Cipriani C, Granberg H, Sassu P, Brånenmark R, Ortiz-Catalan M. Cutting edge bionics in highly impaired individuals: a case of challenges and opportunities. *IEEE Trans Neural Syst Rehabil Eng* 32: 1013–1022, 2024. doi:[10.1109/TNSRE.2024.3366530](https://doi.org/10.1109/TNSRE.2024.3366530).
- Earley EJ, Ortiz-Catalan M. Neurostimulation Perception Obey Strength-Duration Curves and is Primarily Driven by Pulse Amplitude. In: 2023 11th International IEEE/EMBS Conference on Neural Engineering (NER), p. 1–5, 2023. doi:[10.1109/NER52421.2023.10123893](https://doi.org/10.1109/NER52421.2023.10123893).

23. **Ackerley R, Backlund Wasling H, Ortiz-Catalan M, Bränemark R, Wessberg J.** Case Studies in Neuroscience: sensations elicited and discrimination ability from nerve cuff stimulation in an amputee over time. *J Neurophysiol* 120: 291–295, 2018. doi:[10.1152/jn.00909.2017](https://doi.org/10.1152/jn.00909.2017).
24. **Baumgardt E.** Visual spatial and temporal summation. *Nature* 184: 1951–1952, 1959. doi:[10.1038/1841951a0](https://doi.org/10.1038/1841951a0).
25. **Howarth Cl, Lowe G.** Statistical detection theory of Piper's law. *Nature* 212: 324–326, 1966. doi:[10.1038/212324a0](https://doi.org/10.1038/212324a0).
26. **Nie H, Graven-Nielsen T, Arendt-Nielsen L.** Spatial and temporal summation of pain evoked by mechanical pressure stimulation. *Eur J Pain* 13: 592–599, 2009. doi:[10.1016/j.ejpain.2008.07.013](https://doi.org/10.1016/j.ejpain.2008.07.013).
27. **Sloan LL.** Area and luminance of test object as variables in examination of the visual field by projection perimetry. *Vision Research* 1: 121–IN2, 1961. doi:[10.1016/0042-6989\(61\)90024-4](https://doi.org/10.1016/0042-6989(61)90024-4).
28. **Wilson ME.** Invariant features of spatial summation with changing locus in the visual field. *J Physiol* 207: 611–622, 1970. doi:[10.1113/jphysiol.1970.sp009083](https://doi.org/10.1113/jphysiol.1970.sp009083).
29. **Scholtes AMW, Bouman MA.** Psychophysical experiments on spatial summation at threshold level of the human peripheral retina. *Vision Res* 17: 867–873, 1977. doi:[10.1016/0042-6989\(77\)90131-6](https://doi.org/10.1016/0042-6989(77)90131-6).
30. **Kantorovich LV.** *Mathematical Methods of Organizing and Planning Production*. Leningrad State University, 1939.
31. **Vaserstein LN.** Markov processes over denumerable products of spaces, describing large systems of automata. *Problemy Peredachi Informatsii* 5: 64–72, 1969.
32. **Duong LR, Zhou J, Nassar J, Berman J, Olieslagers J, Williams AH.** Representational dissimilarity metric spaces for stochastic neural networks (Preprint). *arXiv*: 1–35, 2022. doi:[10.48550/arXiv.2211.11665](https://doi.org/10.48550/arXiv.2211.11665).
33. **Chappell D, Yang Z, Son HW, Bello F, Kormushev P, Rojas N.** Towards instant calibration in myoelectric prosthetic hands: a highly data-efficient controller based on the Wasserstein distance. *IEEE Int Conf Rehabil Robot* 2022: 25–29, 2022. doi:[10.1109/icrr55369.2022.9896480](https://doi.org/10.1109/icrr55369.2022.9896480).
34. **Fryar CD, Gu Q, Ogden CL.** Anthropometric reference data for children and adults; United States, 2007–2010. *Natl Health Stat Rep* 11, 2012.
35. **Gordon CC, Blackwell CL, Bradtmiller B, Parham JL, Barrientos P, Paquette SP, Corner BD, Carson JM, Venezia JC, Kristensen S.** 2012 anthropometric survey of U.S. Army personnel: methods and summary statistics. U.S. Army Natick Soldier Research Development and Engineering Center, 2014.
36. **The Mathworks I.** fmincon, 2022. In: *Optimization Toolbox*.
37. **The SciPy Developers.** scipy.stats.wasserstein_distance_nd, 2024. In: SciPi.
38. **Schuhmacher D.** wasserstein. In: *transport Package*, 2024.
39. **Nielsen LA, Henriksson KG.** Pathophysiological mechanisms in chronic musculoskeletal pain (fibromyalgia): the role of central and peripheral sensitization and pain disinhibition. *Best Pract Res Clin Rheumatol* 21: 465–480, 2007. doi:[10.1016/j.berh.2007.03.007](https://doi.org/10.1016/j.berh.2007.03.007).
40. **Jin Q, Chang Y, Lu C, Chen L, Wang Y.** Referred pain: characteristics, possible mechanisms, and clinical management. *Front Neurol* 14: 1104817, 2023. doi:[10.3389/fneur.2023.1104817](https://doi.org/10.3389/fneur.2023.1104817).
41. **Forstenpointner J, Otto J, Baron R.** Individualized neuropathic pain therapy based on phenotyping: are we there yet? *Pain* 159: 569–575, 2018. doi:[10.1097/j.pain.0000000000001088](https://doi.org/10.1097/j.pain.0000000000001088).
42. **Ramaswamy S, Wodehouse T.** Conditioned pain modulation—a comprehensive review. *Neurophysiol Clin* 51: 197–208, 2021. doi:[10.1016/j.neucli.2020.11.002](https://doi.org/10.1016/j.neucli.2020.11.002).
43. **Sommerfeld M, Schrieber J, Zemel Y, Munk A.** Optimal transport: Fast probabilistic approximation with exact solvers. *Journal of Machine Learning Research* 20: 1–23, 2019.
44. **Altschuler J, Weed J, Rigollet P.** Near-linear time approximation algorithms for optimal transport via Sinkhorn iteration. In: *NIPS'17: Proceedings of the 31st International Conference on Neural Information Processing System*: 1961–1971, 2017.
45. **Eich E, Reeves JL, Jaeger B, Graff-Radford SB.** Memory for pain: relation between past and present pain intensity. *Pain* 23: 375–380, 1985. doi:[10.1016/0304-3959\(85\)90007-7](https://doi.org/10.1016/0304-3959(85)90007-7).
46. **Salovey P, Smith AF, Turk DC, Jobe JB, Willis GB.** The accuracy of memory for pain. *APS Journal* 2: 184–191, 1993. doi:[10.1016/S1058-9139\(05\)80087-7](https://doi.org/10.1016/S1058-9139(05)80087-7).
47. **Hølen JC, Hjermstad MJ, Loge JH, Fayers PM, Caraceni A, De Conno F, Forbes K, Fürst CJ, Radbruch L, Kaasa S.** Pain assessment tools: is the content appropriate for use in palliative care? *J Pain Symptom Manage* 32: 567–580, 2006. doi:[10.1016/j.jpainsymman.2006.05.025](https://doi.org/10.1016/j.jpainsymman.2006.05.025).
48. **Stevens SS.** To honor fechner and repeal his law. *Science* 133: 80–86, 1961. doi:[10.1126/science.133.3446.80](https://doi.org/10.1126/science.133.3446.80).
49. **Poulton EC.** The new psychophysics: Six models for magnitude estimation. *Psychological Bulletin* 69: 1–19, 1968. doi:[10.1037/h0025267](https://doi.org/10.1037/h0025267).
50. **Mohar B, Ganmor E, Lampl I.** Faithful representation of tactile intensity under different contexts emerges from the distinct adaptive properties of the first somatosensory relay stations. *J Neurosci* 35: 6997–7002, 2015. doi:[10.1523/JNEUROSCI.4358-14.2015](https://doi.org/10.1523/JNEUROSCI.4358-14.2015).
51. **Triscoli C, Croy I, Steudte-Schmiedgen S, Olausson H, Sailer U.** Heart rate variability is enhanced by long-lasting pleasant touch at CT-optimized velocity. *Biol Psychol* 128: 71–81, 2017. doi:[10.1016/j.biopsych.2017.07.007](https://doi.org/10.1016/j.biopsych.2017.07.007).
52. **Marquand A, Howard M, Brammer M, Chu C, Coen S, Mourão-Miranda J.** Quantitative prediction of subjective pain intensity from whole-brain fMRI data using Gaussian processes. *Neuroimage* 49: 2178–2189, 2010. doi:[10.1016/j.neuroimage.2009.10.072](https://doi.org/10.1016/j.neuroimage.2009.10.072).
53. **Williams AH.** A Short Introduction to Optimal Transport and Wasserstein Distance, 2020. <http://alexhwilliams.info/itsneuronalblog/2020/10/09/optimal-transport/>.